Ethylene glycol as an efficient and reversible liquid-organic hydrogen carrier

You-Quan Zou, Niklas von Wolff, Aviel Anaby, Yinjun Xie, David Milstein

Ethylene Glycol as an Efficient and Reversible Liquid Organic Hydrogen Carrier

You-Quan Zou, Niklas von Wolff, Aviel Anaby, Yinjun Xie, David Milstein*.

Department of Organic Chemistry, Weizmann Institute of Science, Rehovot 76100, Israel.

*Correspondence to: david.milstein@weizmann.ac.il (D.M.).

Abstract

Hydrogen has long been regarded as an ideal alternative clean energy vector to overcome the drawbacks of fossil technology. However, the direct utilization of hydrogen is challenging, due to low volumetric energy density of hydrogen gas and potential safety issues. Herein, we report an efficient and reversible liquid to liquid organic hydrogen carrier system based on inexpensive, readily available and renewable ethylene glycol. This hydrogen storage system enables the efficient and reversible loading and discharge of hydrogen using a ruthenium pincer complex, with a theoretical hydrogen storage capacity of 6.5 wt%.

Main Text

The process of industrialization has brought prosperity and wealth to large parts of humanity during the last centuries. However, one fundamental obstacle associated with these processes is the ever-increasing exhaustion of fossil resources, along with the generation of waste and emissions. This directly has an adverse environmental impact (*1*) that might drastically threaten global living conditions in the future. The search for alternative and sustainable energy systems to replace the current fossil fuel-based technologies has thus become one of the central scientific challenges of our society (*2*). In this context, hydrogen has long been regarded as an ideal alternative clean energy vector, which possesses an extremely high gravimetric energy density (lower heating value: 33.3 kWh/kg) and produces water as the sole byproduct upon combustion (*3*). These intrinsic properties of hydrogen make it a particularly attractive candidate for both stationary and mobile applications.

The idea of using hydrogen as energy source and carrier can be dated back to the late 20th century. One of the earliest perspectives on this subject was proposed by Jones in 1971 (*4*). He pointed out that "using liquid hydrogen must be seriously considered as the logical replacement for hydrocarbon fuels in the 21st century". The concepts of hydrogen economy and hydrogen storage were specified by Bockris in 1972 (*5*). Shortly after, Winsche and co-workers also postulated that "a hydrogen fuel economy would be of major interest as an alternative to a predominated electric economy in the future" (*6*). Recently, significant advances have been made in hydrogen-powered fuel cells (*7*). Nonetheless, hydrogen as energy vector has not yet been universally applied, and problems related to its storage and transport still exist. Efficient storage of hydrogen is both crucial and challenging, due to its low volumetric energy density. Traditionally, hydrogen is stored physically in gas tanks under high pressure (*8*) or as a liquid (*9*)

at cryogenic temperatures. However, the high energy input needed for storage, the low volumetric energy density, and potential safety issues largely limit applications using molecular hydrogen. Although extensive efforts have been made to store hydrogen in nanostructured materials, metal organic frameworks and metal hydrides (*10, 11*), these systems suffer from low hydrogen storage capacities (HSC), harsh conditions, low energy efficiency, and high cost.

In contrast, storing hydrogen in chemical bonds of small organic molecules, especially organic liquids, has received considerable research interests during the last few years (*12, 13*). The usage of a proper catalytic system would allow for the efficient release of hydrogen by promoting the dehydrogenation reaction, and recovery of the hydrogen depleted substance by hydrogenation. In this scenario, methanol (*14-17*), formaldehyde (*18, 19*), or formic acid (*20-22*) are frequently introduced as hydrogen carriers. Nevertheless, factors such as CO_2 release, (e.g., methanol and formaldehyde), toxicity, and low hydrogen storage capacity of formic acid (4.4 wt%) limit these approaches. Therefore, the development of novel and reversible hydrogen storage systems with satisfying economic and ecological benefits is highly desirable. In this regard, liquid organic hydrogen carriers (LOHC) have emerged as a unique and powerful tool to advance this goal (*23-26*), wherein a pair of hydrogen-rich and hydrogen-deficient organic liquids can repeatedly discharge and load hydrogen *via* reversible and catalytic dehydrogenation and hydrogenation cycles (Fig. 1a). Ideally, LOHC would feature high safety and purity, low cost, easy transport, and reversibility, and would be compatible with the existing infrastructure for fossil fuels as liquid energy vectors. Importantly, in order for LOHC systems to become economically viable, the European Union and the US government set HSC goals of 5.0 wt% and 5.5 wt%, respectively (*27, 28*). This paradigm was exemplified in a hydrogen storage system based on dodecahydro-*N*-ethylcarbazole (H12-NEC) and *N*-ethylcarbazole (NEC) (*29*) with a HSC as high as 5.8 wt%, (Fig.

1b). Due to the favorable dehydrogenation thermodynamics (e.g., compared to cycloalkanes) (*30*), liquid organic hydrogen carriers are continuously dominated by *N*-containing heterocycles (*23-26, 31, 32*), which nevertheless require high temperatures (which often result in decomposition products) and pressures for the catalytic process to be efficient. On the other hand, our group and the Prakash group have developed several LOHC systems through dehydrogenative formation of amides (*33*) and their hydrogenation, starting from ethanolamine (*34*), ethanol-ethylenediamine (*35*), 1,4-butanediol-ethylenediamine (*36*) or methanol-ethylenediamine (*37*), respectively. In most cases, the amides (hydrogen-deficient compounds) are formed as solids from the dehydrogenative coupling of amines and alcohols. An ideal LOHC system would feature both the hydrogen-rich and hydrogen-deficient organic compounds as liquids. Therefore, the search for novel and reversible liquid to liquid hydrogen storage systems based on inexpensive, green, renewable and abundant organic liquids with high hydrogen capacities is challenging and still to be accomplished. Here we report a liquid organic hydrogen carrier system based on the inexpensive, widely accessible and renewable ethylene glycol, capable of chemically storing and releasing hydrogen reversibly using the same catalyst, with a theoretical hydrogen storage capacity of 6.5 wt%.

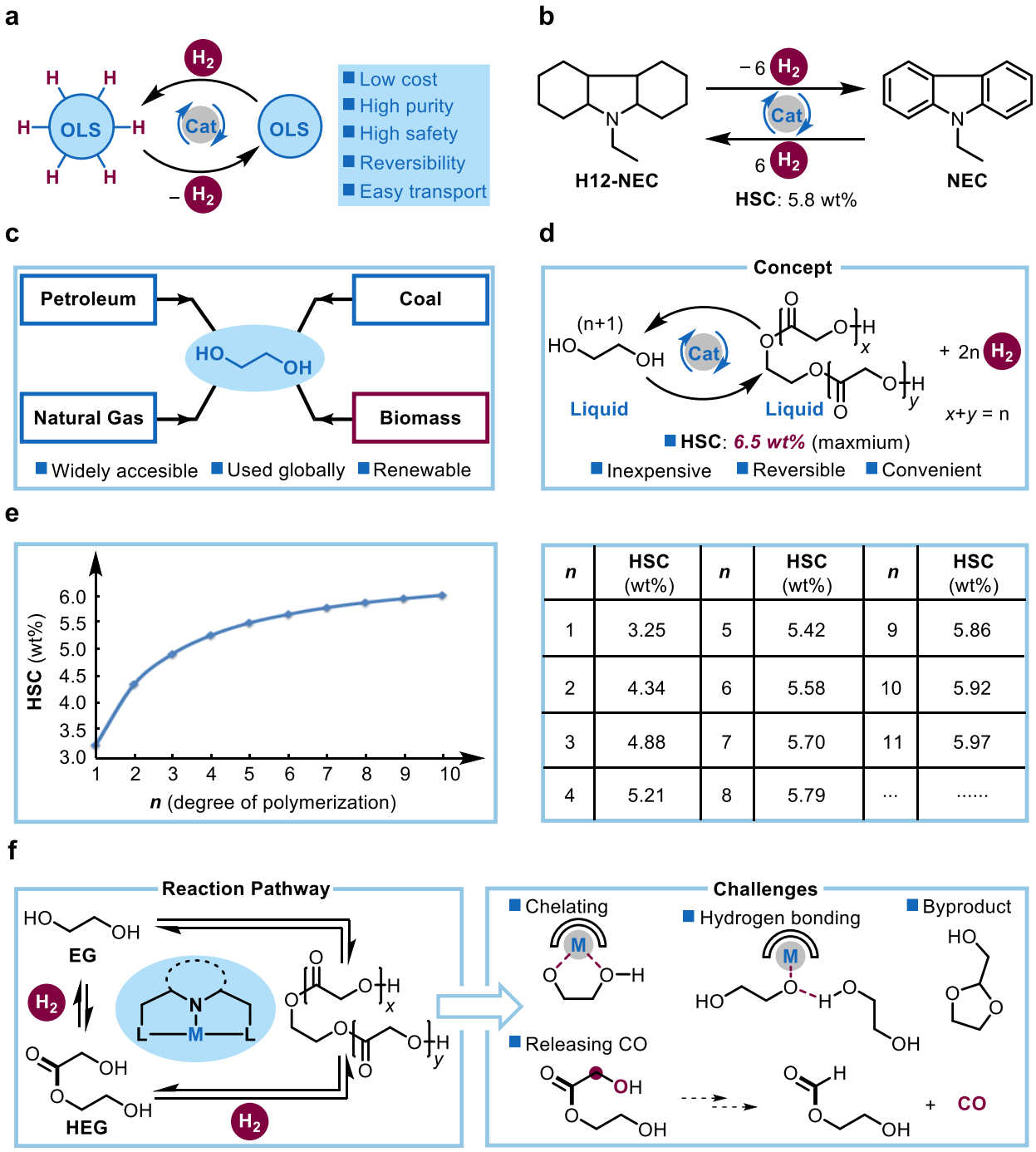

n	HSC (wt%)	*n*	HSC (wt%)	*n*	HSC (wt%)
1	3.25	5	5.42	9	5.86
2	4.34	6	5.58	10	5.92
3	4.88	7	5.70	11	5.97
4	5.21	8	5.79	···	·····

Fig. 1. Development of a liquid organic hydrogen carrier system based on ethylene glycol. a, General concept of liquid organic hydrogen carrier. OLS, organic liquids; Cat, catalyst. **b**, Well-established liquid organic hydrogen carrier based on *N*-ethylcarbazole. NEC, *N*-ethylcarbazole. **c**, Methods for producing ethylene glycol. **d**, Concept and advantages using ethylene glycol as a

liquid organic hydrogen carrier. HSC, hydrogen storage capacity. **e**, Hydrogen storage capacity versus degree of polymerization based on ethylene glycol. **f**, Possible reaction pathways for dehydrogenation and reverse hydrogenation using ethylene glycol and hypothesized challenges. EG, ethylene glycol; HEG, 2-hydroxyethyl glycolate.

Results

Design plan. Ethylene glycol (EG), a widely accessible odorless, colorless, viscous liquid, represents the simplest vicinal diol. EG is used globally, with more than 34 million tons global production capacity in 2016 (*38, 39*). For instance, it is a vital component in antifreeze and coolant systems in automobiles, and in deicing fluids for windshields and aircrafts (*38, 39*). Moreover, it is extensively applied in the manufacturing of polyester fibers and resins (*38, 39*), such as polyethylene terephthalate (PET). Importantly, ethylene glycol is not only derived from fossil resources, but also from biomass-derived hydrocarbons (*40*) (Fig. 1c), highlighting its potential as a sustainable resource. Given that EG is an inexpensive, renewable, and already an industrially applied product, makes it a promising candidate for LOHC applications. Literature precedents show that EG is indeed suitable for liberating hydrogen in the presence of water under heterogeneous conditions (*41, 42*). Nevertheless, the closing of the charge/discharge cycle by hydrogenation to reform EG has not been achieved, since competitive pathways are at play forming hydrogen, carbon dioxide and gaseous alkanes (C1-C2) as side-products. In 2005, our group disclosed an efficient acceptorless dehydrogenative coupling of alcohols catalyzed by a ruthenium pincer complex *via* metal-ligand cooperation, enabling access to a wide range of esters with release of hydrogen under mild conditions (*43*). A year later the homogeneously catalyzed hydrogenation of esters under low pressure was reported (*44*). Since then, significant works have been reported, highlighting the generalizability of these processes to different substrates (*45-47*). We envisioned

that ethylene glycol (hydrogen-rich organic liquid) might undergo dehydrogenative esterification reactions to liquid oligoesters (hydrogen-deficient organic liquid), which may then be reversibly hydrogenated to ethylene glycol (Fig. 1d). The successful implementation of this cycle can provide a novel LOHC system with a maximum theoretical HSC of 6.5 wt%, which is above the targets set for 2020 by the European Union (5.0 wt%) (*27*) and the U.S. Department of Energy (5.5 wt%) (*28*). Plotting the evolution of HSC with the degree of polymerization clearly shows that high HSC can be obtained already from pentamer (*i.e.* above 5.21 wt%, HSC = $(2n \times M_{H2})/[(n+1) \times M_{EG}]$, M_{H2}: molar mass of hydrogen (2.02 g/mol), M_{EG}: molar mass of ethylene glycol (62.07 g/mol)), and full conversion to high molecular weight polymers is not necessary to achieve the goals set for 2020 (Fig. 1e).

The proposed reaction pathway is outlined in Fig. 1f. Initially, two molecules of EG are coupled to 2-hydroxyethyl glycolate (HEG), catalyzed by a metal pincer complex accompanied by the release of two equivalents of hydrogen. Subsequently, HEG can react with additional equivalents of EG to afford higher oligomers in a similar fashion. As pointed out, HSC increases with an increase of oligomerization and liberation of H_2. For a hydrogen storage system, hydrogenation of the resulting oligomers back to EG should be possible, ideally using the same catalyst. Nevertheless, the acceptorless catalytic dehydrogenative coupling to even HEG is highly challenging. Possible drawbacks that might explain the reluctance of EG to undergo the desired transformation might include: 1) EG chelates the metal center of the pincer complex and hampers catalyst activity; 2) hydrogen bonding between a possible alkoxy metal complex and neighboring EG may hinder β-hydride elimination steps, preventing generation of the aldehyde intermediate; 3) HEG can be dehydrogenated to α-keto ester upon the oxidation of the α-hydroxyl group, which would easily decompose to CO and aldehyde, with subsequent CO poisoning of the catalyst; 4)

undesired formation of cyclic side products ((1,3-dioxolan-2-yl)methanol) with lower hydrogen capacities. In order to establish EG as an elegant and performing LOHC, these challenges have to be circumvented efficiently. Herein we report an unprecedent, inexpensive, convenient and reversible LOHC system based on acceptorless dehydrogenative esterification of EG and hydrogenation of the corresponding oligoesters.

Acceptorless dehydrogenative coupling of ethylene glycol. To test the feasibility of the acceptorless dehydrogenative coupling of EG, we began our investigation by evaluating the PNNH ruthenium complexes **Ru-1**, **Ru-2** and **Ru-3** (1 mol% loading) in the presence of 2 mol% potassium *tert*-butoxide (^{t}BuOK) in refluxing toluene at 135 °C (bath temperature) for 48 hours. Reaction monitoring showed very sluggish conversions, which may be due to the low solubility of EG in toluene (Table 1, entries 1-3). Indeed, the conversions could be increased to 53% in more polar solvents and 18 mL hydrogen were collected within 24 hours by using **Ru-3** as the catalyst and 2.0 mmol ethylene glycol in 1,2-dimethoxy ethane (DME) (Table 1, entries 4-6). Using a mixture of toluene and DME (v/v = 1:1) at 135 °C, the reaction efficiency was further improved to 56% (Table 1, entry 7). Elevating the temperature to 150 °C led to 83% conversion and 44 mL hydrogen after 72 hours (Table 1, entry 8). Higher degrees of oligoesters were observed *via* nuclear magnetic resonance (NMR) spectroscopy (Supplementary Figure 22) and mass spectrometry (MS) (Supplementary Figure 47) of the reaction mixture, with HEG as the major product. Examining the gas phase by gas chromatography (GC) showed that the purity of hydrogen was 99.57% (Supplementary Figure 50). Screening other reaction parameters such as concentration (e.g., 0.25 M, 2 M, 4 M; Table 1, entries 8-11), base (e.g., ^{t}BuONa, ^{t}BuOLi; Table 1, entries 12-13) and other mixed solvents (e.g., toluene/1,4-dioxane, toluene/diglyme; Table 1, entries 14-15) revealed that 1 M solution, ^{t}BuOK, and a solvent toluene/DME (v/v = 1:1) gave the best results. We then re-

investigated the activity of complexes **Ru-1** and **Ru-2** using the mixed solvent system, with **Ru-3** still giving the best results (Fig. 2a).

Table 1. Optimization of reaction conditions using PNNH complexes Ru-1 to Ru-3.

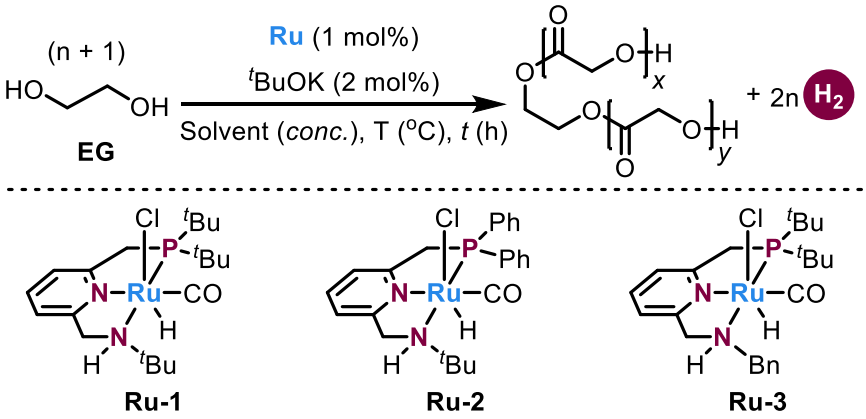

entry[a]	Ru	Solvent (*conc.*)	T (˚C)	*t* (h)	conv. (%)[b]	V (H_2, mL)
1	**Ru-3**	toluene (1.0 M)	135	48	23	10
2	**Ru-1**	toluene (1.0 M)	135	48	3	~1
3	**Ru-2**	toluene (1.0 M)	135	48	8	~1
4	**Ru-3**	THF (1.0 M)	135	24	50	16
5	**Ru-3**	dioxane (1.0 M)	135	24	41	16
6	**Ru-3**	DME (1.0 M)	135	24	53	18
7	**Ru-3**	toluene/DME (1.0 M)	135	72	56	24
8	**Ru-3**	**toluene/DME (1.0 M)**	**150**	**72**	**83**	**44**
9[c]	**Ru-3**	toluene/DME (0.25 M)	150	72	48	14
10	**Ru-3**	toluene/DME (2.0 M)	150	72	78	42
11	**Ru-3**	toluene/DME (4.0 M)	150	72	73	35
12[d]	**Ru-3**	toluene/DME (1.0 M)	150	72	66	32
13[e]	**Ru-3**	toluene/DME (1.0 M)	150	72	40	19

14	**Ru-3**	toluene/dioxane (1.0 M)	150	72	79	41
15	**Ru-3**	Toluene/diglyme (1.0 M)	150	72	51	21

[a]Reaction conditions: ethylene glycol (2.0 mmol), Ru cat. (1 mol%), ^{t}BuOK (2 mol%), solvent (2.0 mL) or mixed solvent (2.0 mL, v/v = 1:1) at 135 or 150 °C (bath temperature) for 24–72 hours. [b]Conversions were determined by ^{1}H NMR from the reaction mixture using mesitylene as an internal standard. [c]1.0 mmol Ethylene glycol was used. [d] ^{t}BuONa (2 mol%) was used instead of ^{t}BuOK. [e] ^{t}BuOLi (2 mol%) was used instead of ^{t}BuOK. The bold entry denotes the best performance.

In order to further improve the reaction efficiency, we next screened other types of catalysts developed in our group. As shown in Fig. 2b, the PNN ruthenium pincer complexes **Ru-4**, **Ru-5** and **Ru-6** also catalyze this transformation, although with lower conversions (26-43%) and less evolved hydrogen (13-23 mL). Use of the PNP ruthenium complexes **Ru-7** and **Ru-8** drastically slowed down the dehydrogenative reaction (Fig. 2c). Notably, a significant improvement was achieved by using the acridine-based PNP ruthenium complex **Ru-9**. With this system a conversion of 94% was achieved, together with the formation of 54 mL hydrogen (purity: = 99.65%, see Supplementary Table 3, entry 9 and Supplementary Figure 51 for details). Based on NMR spectroscopy of the crude reaction mixture, the yield of HEG was determined to be 33%, with the remaining conversion being due to higher oligoesters (Supplementary Figures 37 and 48).

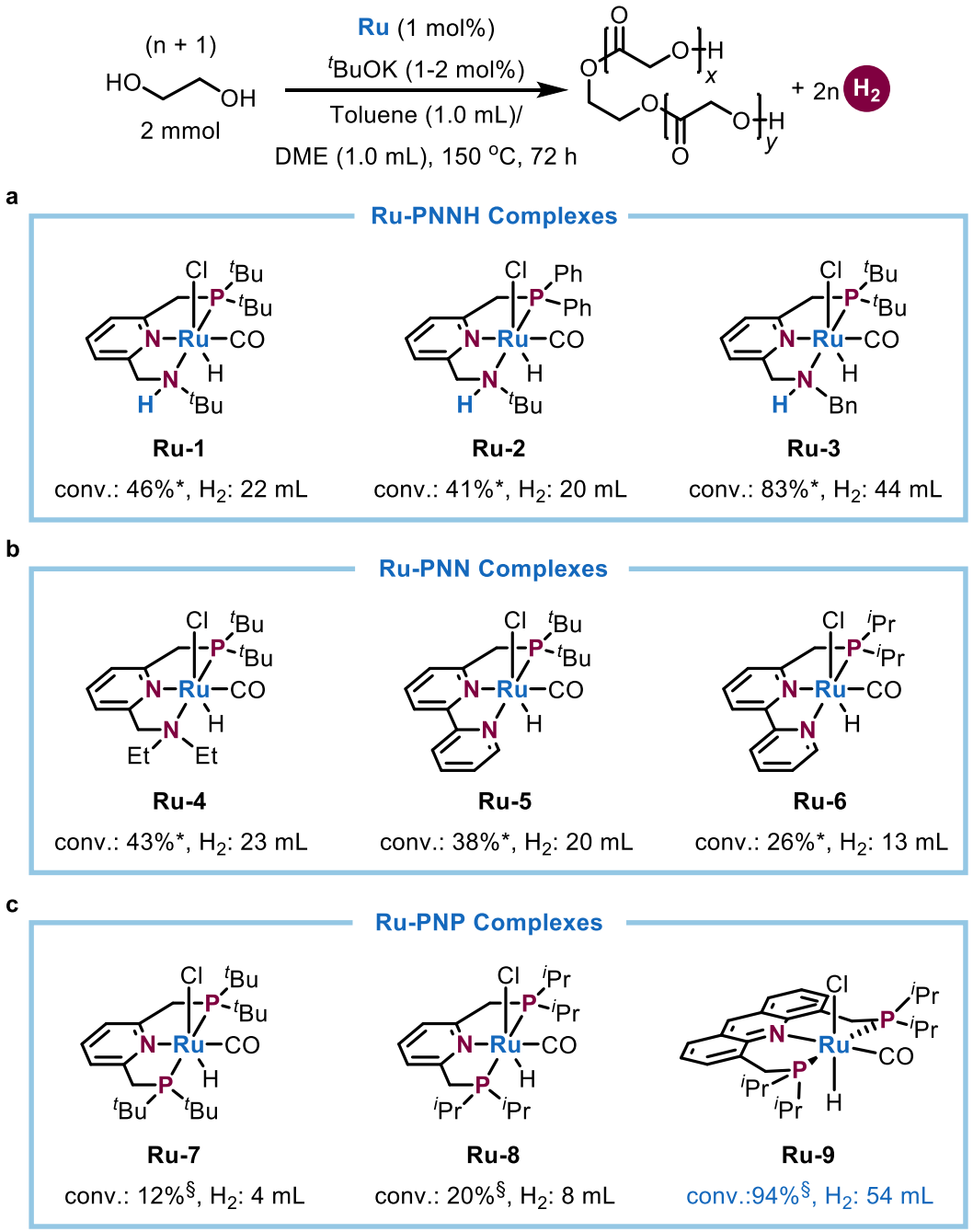

Fig. 2. Results of catalytic acceptorless dehydrogenative coupling of ethylene glycol. Reaction conditions: ethylene glycol (2.0 mmol), ruthenium pincer complex (1 mol%), ^{t}BuOK (1-2 mol%), toluene/DME (1.0 mL /1.0 mL), 150 ˚C, 72 hours. All conversions were determined by ^{1}H NMR

analysis of the reaction mixture using mesitylene as an internal standard. *2 mol% ^{t}BuOK was used. §1 mol% ^{t}BuOK was used.

Encouraged by the results using **Ru-9**, we then considered to use the dearomatized complex **Ru-10** as a catalyst and performed the reaction under base-free conditions. The dehydrogenative coupling of EG proceeded smoothly in the presence of 1 mol% of **Ru-10**, affording substantial improvement over the PNN and PNNH family of ruthenium complexes (97% conversion, 61 mL hydrogen with 99.59% purity, Fig. 3a and Supplementary Figure 52). The yield of hydrogen was 64% referenced to the maximum HSC of EG (6.5 wt%, at high degree of polymerization). Analyzing the reaction mixture showed that higher oligomers (n up to 6) were formed as well (Supplementary Figures 38 and 49). Accordingly, a base-free catalytic system that consists of **Ru-10** (1 mol%) and a mixed solvent of toluene/DME (v/v = 1:1) gave the best performance of the acceptorless dehydrogenative coupling of EG.

Recovery of ethylene glycol. After the encouraging implementation of the acceptorless dehydrogenative coupling of EG, we next explored whether the reverse hydrogenation reaction could be accomplished under similar conditions. In light of an ideal LOHC system, where the same catalyst can be used for both loading and discharging, we then carried out the hydrogenation reactions using complex **Ru-10**. Interestingly, the reaction mixture depicted in Fig. 3A was fully hydrogenated back to EG (92% NMR yield, Supplementary Figure 39) in the presence of 1 mol% of **Ru-10** under 40 bar of hydrogen and a mixed solvent (toluene/DME, v/v = 1:1) within 48 hours (Fig. 3b). Thus, EG and its oligoesters could be interconverted under similar reaction conditions. The above results indicate that a reversible LOHC system based on EG is possible using pincer

complex **Ru-10** as catalyst. The stabilities of **Ru-10** under both dehydrogenation and hydrogenation conditions were also studied, please see Supplementary Method 6 for details.

Neat ethylene glycol under partial vacuum. Solvent-free reaction conditions are advantageous regarding optimal hydrogen capacity of the system, potentially shortened reaction time, reduced energy consumption, and lower capital investment; therefore they are considered more environmentally benign and cost-effective. Hence, a solvent-free LOHC system might be more attractive for industrial applications. Moreover, solvent-free conditions can facilitate polymerization reactions. We thus performed the dehydrogenation reaction of EG on a larger scale (35.9 mmol, 2 mL) under neat conditions at 150 °C and reduced pressure (95 mbar). Under these conditions, 94% conversion was obtained after seven days using 0.5 mol% of **Ru-10** (Fig. 3c). Based on the ^{1}H NMR of the crude reaction mixture it is estimated that 1295 mL of hydrogen were formed, with an average degree of oligomerization of 3.98 (Supplementary Figures 40-42 and 55). It is worth mentioning that the hydrogen yield was further increased to 75% (referenced to the maximum HSC of EG, 6.5 wt%) and the realized HSC was 5.2 wt%. Reduced pressure is used to effectively keep the reaction system under reflux for efficient removal of the generated hydrogen and drive the reaction forward. Moreover, the above crude reaction mixture could be fully hydrogenated back to EG within 60 hours in the presence of 0.5 mol% of **Ru-10** under 40 bar of hydrogen in a mixed toluene/ DME (1 mL / 1 mL) solvent (Supplementary Figure 43).

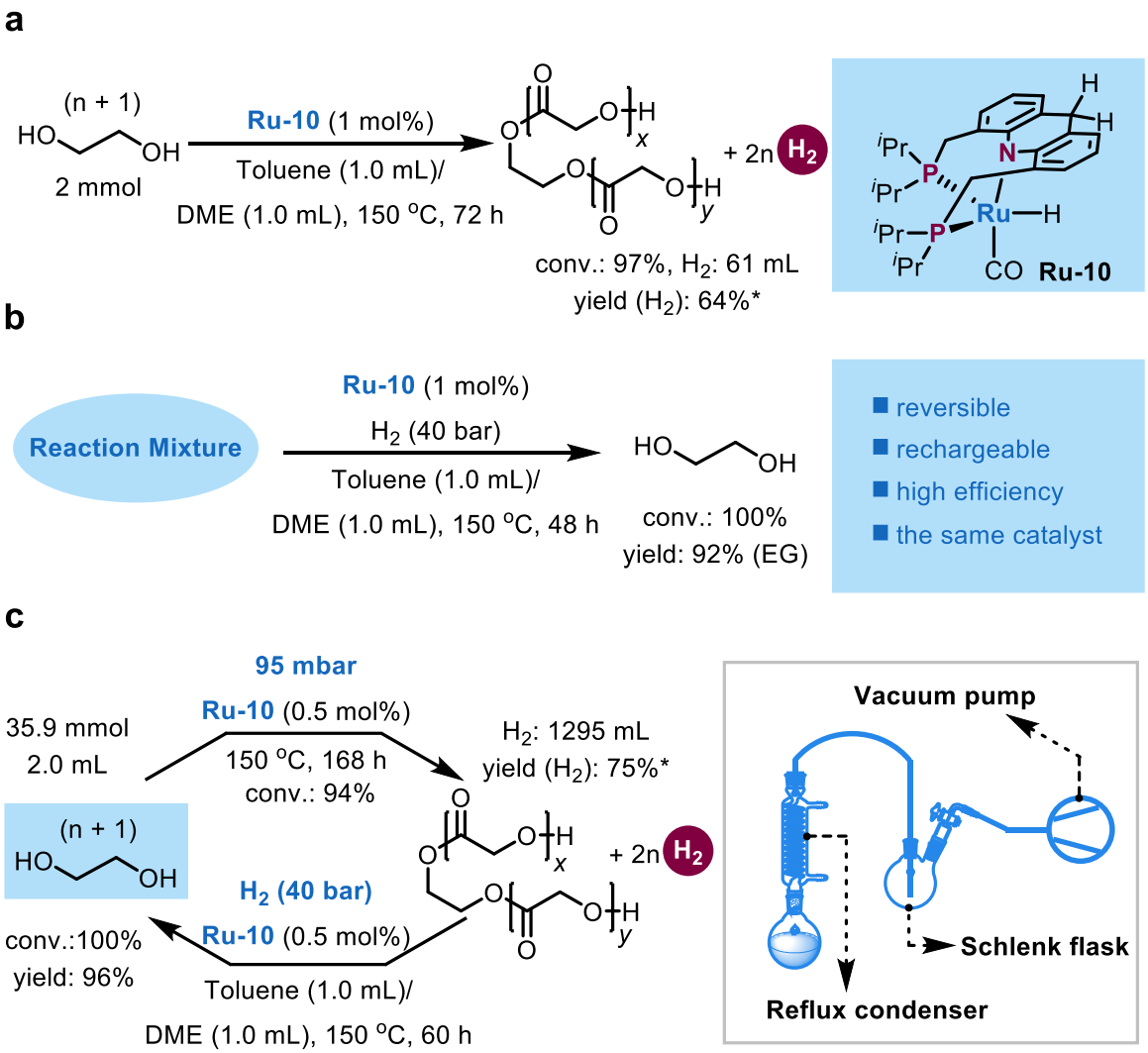

Fig. 3. Results of catalytic acceptorless dehydrogenative coupling of ethylene glycol and hydrogenation of reaction mixture using dearomatized complex 10. a, Acceptorless dehydrogenative coupling of ethylene glycol catalyzed by the dearomatized complex **Ru-10** without base. **b,** Recovery of ethylene glycol by hydrogenation of the reaction mixture. **c,** Large scale reaction performed under partial vacuum without solvent. *The yield of hydrogen is referenced to the maximum HSC of EG, 6.5 wt%.

Mechanistic studies. In order to gain mechanistic insight regarding the reversible dehydrogenation/hydrogenation of EG catalyzed by **Ru-10**, DFT calculations were employed (see supplementary information for details). Importantly, overall the dehydrogenation of EG to HEG is calculated to be very slightly endergonic, ΔG = 0.6 kcal.mol^{-1} (at 423.15 K in the gas phase), highlighting the readily feasible and reversible dehydrogenation/hydrogenation events. The enthalpy of the dehydrogenation of EG to HEG was calculated to ΔH = 9.2 kcal.mol^{-1}. We also calculated the ΔG (and ΔH) for the formation of tetramers, which varies between -7.5 and 8.9 kcal.mol^{-1} (ΔH varies between 18.4 and 32.6 kcal.mol^{-1}) depending on the connectivity and conformation (see Supplementary Figure 64 for details).

In the first step, EG can add to the 5-coordinate complex **Ru-10** yielding intermediate **A** (Fig. 4). This reaction is only slightly downhill in energy (-2.3 kcal.mol^{-1}). Dehydrogenation by protonation of the Ru−H bond *via* $\mathbf{TS_{AB}}$ (24.7 kcal.mol^{-1}) liberates one equivalent of H_2 together with the formation of κ2- alkoxide coordinated **B** (-5.1 kcal.mol^{-1}). Decoordination of the hydroxo group allows for *β*-hydride elimination *via* $\mathbf{TS_{BC}}$ (7.2 kcal.mol^{-1}), and reforms a Ru−H bond in **C** (5.9 kcal.mol^{-1}). With another molecule of EG, **C** undergoes dehydrogenation to **D** (3.7 kcal.mol^{-1}) *via* a concerted Zimmerman-Traxler-like 6-membered transition state ($\mathbf{TS_{CD}}$, 23.4 kcal.mol^{-1}). Importantly, the pathway from **C** to glyoxal (15.7 kcal.mol^{-1}, intermediate **F**, Fig. 5) without addition of EG *via* dehydrogenation ($\mathbf{TS_{CF1}}$, 27.7 kcal.mol^{-1}, Fig. 5) and *β*-hydride elimination ($\mathbf{TS_{CF2}}$, 12.7 kcal.mol^{-1}, Fig. 5) is both kinetically and thermodynamically unfavored. In addition, also the formation of cyclic products from hemiacetals (intermediate I, see Supplementary Figure 61) with lower HSC is avoided by high lying transition states ($\mathbf{TS_{CG}}$ = 45.6 kcal.mol^{-1} and $\mathbf{TS_{HI}}$ = 54.2 kcal.mol^{-1}, see Supplementary Figure 61). Another *β*-hydride elimination event (12.7 kcal.mol^{-1}) from κ2-hemiacetalate **D** gives the metal bound ester **E** (6.8 kcal.mol^{-1}). Finally,

decoordination re-forms the active catalyst **Ru-10** and releases HEG. Noteworthy, the lowest lying intermediate, namely **B**, is only 5.1 kcal.mol^{-1} more stable than the active catalyst **Ru-10**, although **Ru-10** is unsaturated. Again, a higher stabilization is most likely hindered by the strained geometry (equatorial P-Ru-O angles of 160.8° and 165.2° respectively in **B**) and thus prevents a higher energetic span. Moreover, the aromatic acridine backbone is involved in OH-π interactions upon addition of a second EG unit in transition states $\mathbf{TS_{CD}}$ and $\mathbf{TS_{DE}}$ as well as intermediates **D** and **E**. This might not only favor hemiacetalate formation over the glyoxal pathway (Fig. 5) by enabling a H-bond stabilized Zimmerman-Traxler like transition state, but also prevent water elimination from the hemiacetalate upon cyclization by binding the OH-group of the side-arm. This might also prevent extensive hydrogen bonding with non-coordinated EG/HEG in solution. Hence, the unique characteristics of the acridine ligand framework enable **Ru-10** to overcome the challenges outlined in Fig. 1F. Finally, rate-limiting transition states are associated with dehydrogenation events, whereas hydride abstraction is readily achieved (see Supplementary Method 7 for further discussion).

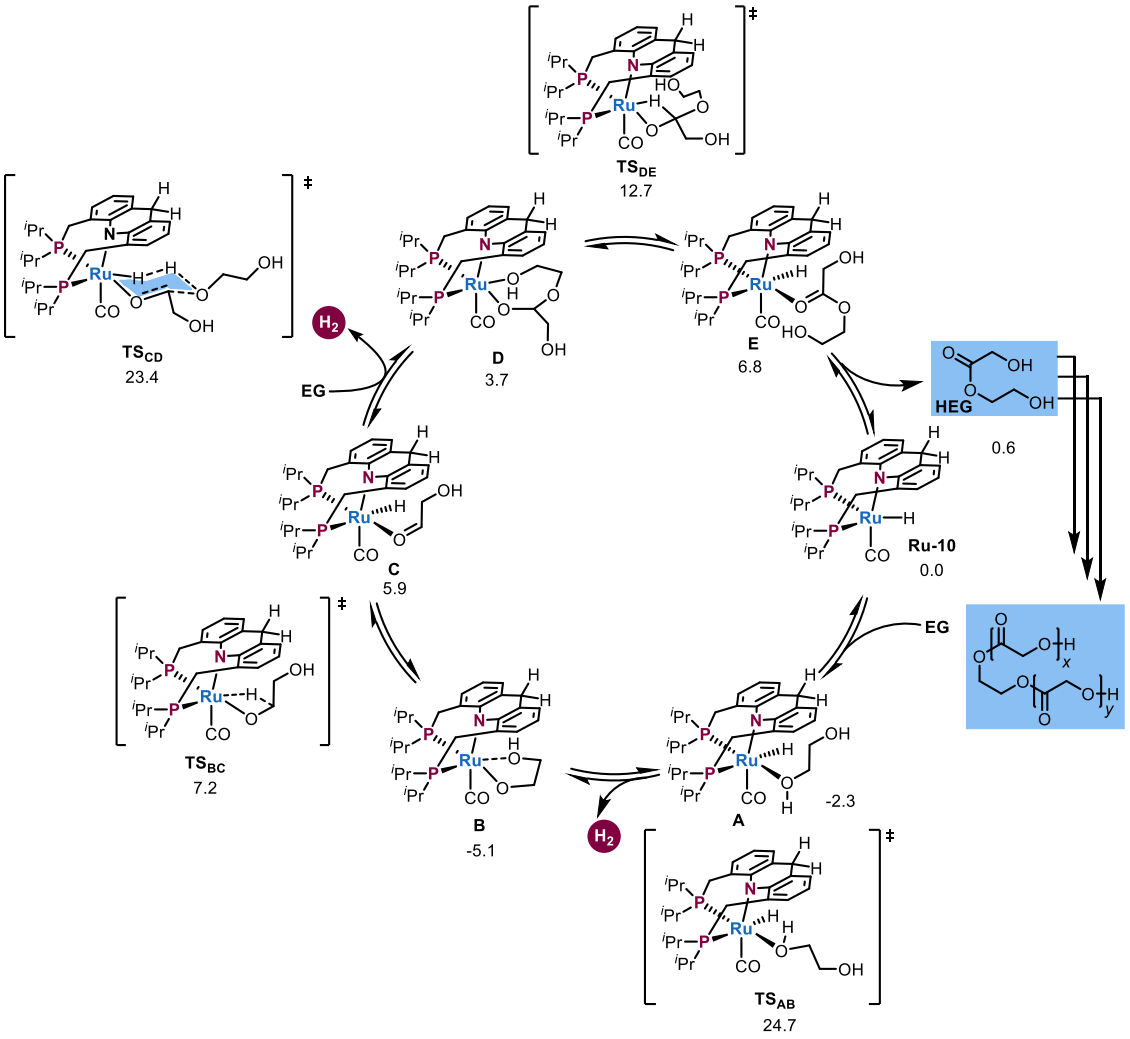

Fig. 4. Proposed catalytic cycle. All values correspond to Gibbs Free Energies at 423.15 K (in kcal.mol^{-1} with respect to the starting material).

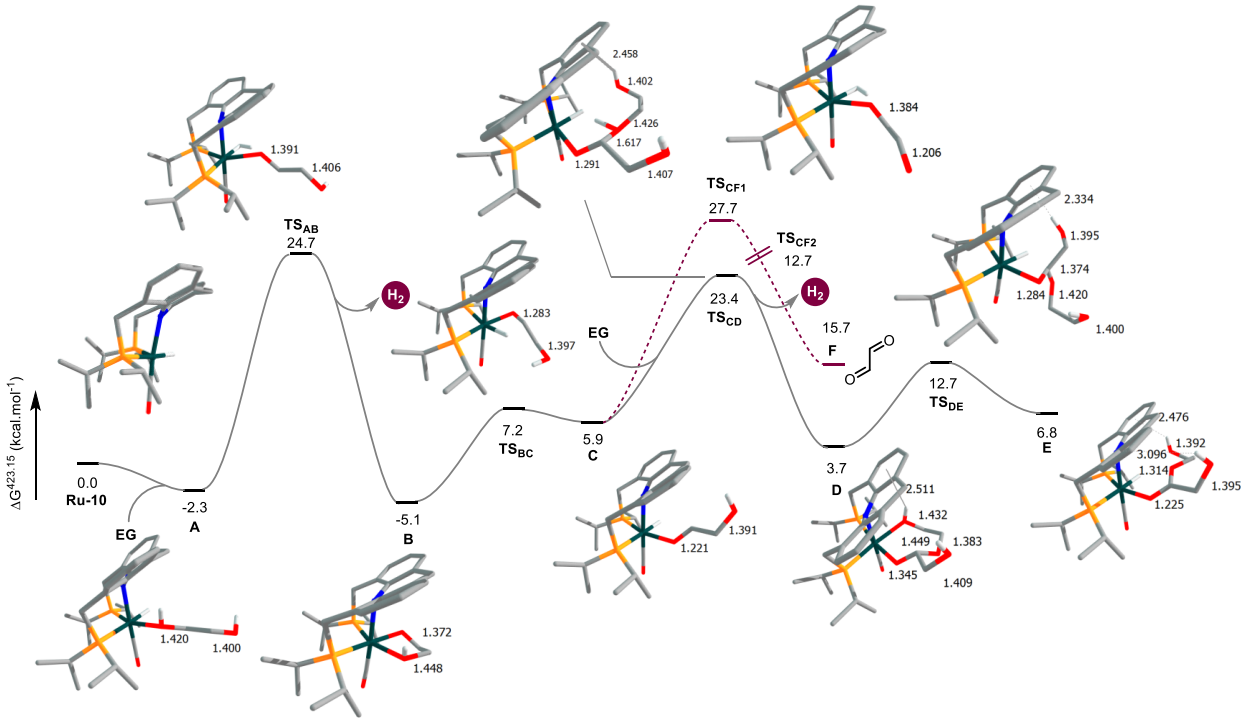

Fig. 5. Energy levels of the proposed catalytic cycle. Values correspond to Gibbs Free Energies (in kcal.mol^{-1} with respect to the starting material) at 423.15 K. Values in structures highlight OH-π interactions (in Å) and distinguish sp^2 from sp^3 C-O bonds. C-H bonds are omitted for clarity.

Conclusion

In conclusion, a convenient and reversible liquid to liquid hydrogen storage system based on inexpensive and renewable EG was developed. This hydrogen storage system can theoretically provide high HSC (6.5 wt%) and hydrogen can be efficiently loaded and discharged by using the same catalyst under similar reaction conditions. The unique characteristics of the acridine ligand-backbone are responsible for overcoming challenges normally related to the usage of EG. We believe that this LOHC system, although not at a practical level yet, might, upon further development, help push forward the development of LOHCs as energy vectors for large-scale applications, such as in transportation and in energy storage, and might thus help lay the

groundwork for a more sustainable economy in the future. Further development of this system is in progress.

Methods

General procedure for dehydrogenative coupling of EG using a mixed solvent. In a glovebox, ethylene glycol (124.1 mg, 2.0 mmol) was added with a glass pipette into a 100 mL Schlenk tube equipped with a magnetic stirring bar. A 5 mL vial containing a magnetic stirring bar was charged with ruthenium pincer complex **Ru** (0.02 mmol), ^{t}BuOK (0.02 – 0.04 mmol) and THF (1.0 mL). The mixture was stirred at room temperature for 10 min, followed by removing the solvent under vacuum. The residue was dissolved in dry and degassed toluene (2 × 0.5 mL) and the solution was transferred into the above Schlenk tube using the same glass pipette. The vial was washed with solvent **2** (2 × 0.5 mL) and the solution was transferred into the Schlenk tube. The Schlenk tube was taken out of the glovebox and stirred at 135 ˚C or 150 ˚C for the specified hours. Then the reaction mixture was firstly cooled to room temperature, and then the Schlenk tube was connected to the gas collecting system to measure the volume of gas. Finally, the solvent was removed under vacuum, mesitylene (139 μL, 1.0 mmol) was added into Schlenk tube as an internal standard. The residue was dissolved in d6-Acetone, and the resulting solution was passed through a short Celite column and then submitted to NMR analysis.

General procedure for dehydrogenative coupling of EG without base. In a glovebox, ethylene glycol (124.1 mg, 2.0 mmol) was added into a 100 mL Schlenk tube equipped with a magnetic stirring bar through a glass pipette. A 5 mL vial containing a magnetic stirring bar was charged with ruthenium pincer complex **Ru-10** (0.02 mmol) and dry and degassed toluene (1.0 mL) and the solution was transferred into the above Schlenk tube using the same glass pipette. The vial was

washed with dimethoxyethane (DME, 2 × 0.5 mL) and the solution was transferred into the Schlenk tube. The Schlenk tube was taken out of the glovebox and stirred at 150 ˚C for 72 hours. Then the reaction mixture was firstly cooled to room temperature, and then the Schlenk tube was connected to the gas collecting system to measure the volume of gas (61 mL gas was collected in total). Finally, the solvent was removed under vacuum, mesitylene (139 μL, 1.0 mmol) was added into Schlenk tube as an internal standard. The residue was dissolved in d*6*-Acetone, and the resulting solution was passed through a short Celite column and then submitted to NMR analysis. ^{1}H NMR indicated that the conversion was 97%.

General procedure for reversible hydrogenation of the reaction mixture. In a glovebox, a 25 mL stainless steel autoclave with a Teflon tube containing a magnetic stirring bas was charged with **Ru-10** (0.02 mmol). The dehydrogenated reaction mixture in a 5 mL vial was dissolved in dry and degassed toluene (2 × 0.5 mL) and the solution was transferred into the Teflon tube of the autoclave. The vial was washed with dimethoxyethane (DME, 2 × 0.5 mL) and the solution was transferred into the Teflon tube of the autoclave. The autoclave was taken out of the glovebox and purged five times with hydrogen and finally pressurized to 40 bar. The reaction mixture was stirred at 150 ˚C (oil bath temperature) for 48 hours, and then was cooled to room temperature in an ice bath. Then the reaction mixture was transferred into a 25 mL vial and the solvent was removed under vacuum, mesitylene (139 μL, 1.0 mmol) was added into Schlenk tube as an internal standard. The residue was dissolved in d*6*-Acetone, and the resulting solution was passed through a short Celite column and then submitted to NMR analysis. ^{1}H NMR indicated that the conversion was 100% and the yield of ethylene glycol was 92%.

Computational method. Computed energies and cartesian coordinates of the optimized intermediates and transition states, as well as additional details and references can be found in the Supplementary Data. In short, all structures were optimized at the M06-L/Def2-SVP/W06/GD3 level of theory using Gaussian16 (B.01). Frequency calculations at 423.15 K confirmed stationary points and transition states (one imaginary frequency) and were used to obtain thermochemical corrections. Single point energy calculations at the ωB97X-V/Def2-TZVP/JKFIT on the optimized structures were used to obtain ΔG values (together with the thermochemical corrections) using the open-source PSI4 (1.2.1 release) package. The range-separated hybrid GGA ωB97X-V functional was recently shown to give excellent results in a thermochemical benchmark set of metal organic reactions (*48*), rationalizing its usage.

Data Availability.

The data that support the findings of this study are available from the corresponding author upon reasonable request.

References

1. M. Höök, T. Xu, Depletion of fossil fuels and anthropogenic climate change – a review. *Energy Policy* **52**, 797–809 (2013).
2. S. Chu, A. Majumdar, Opportunities and challenges for a sustainable energy future. *Nature* **488**, 294–303 (2012).
3. D. A. J. Rand, R. M. Dell, *Hydrogen Energy: Challenges and Prospects* (RSC Publishing, Cambridge, 2007).
4. L. W. Jones, Liquid hydrogen as a fuel for the future. *Science* **174**, 367–370 (1971).

5. J. O'M. Bockris, A hydrogen economy. *Science* **176**, 1323 (1972).

6. W. E. Winsche, K. C. Hoffman, F. J. Salzano, Hydrogen: its future role in the nation's energy economy. *Science* **180**, 1325–1332 (1973).

7. B. C. H. Steele, A. Heinzel, Materials for fuel-cell technologies. *Nature* **414**, 345–352 (2001).

8. U. Eberle, B. Müller, R. von Helmolt, Fuel cell electric vehicles and hydrogen infrastructure: status 2012. *Energy Environ. Sci.* **5**, 8780–8798 (2012).

9. M. S. Sadaghiani, M. Mehrpooya, Introducing and energy analysis of a novel cryogenic hydrogen liquefaction process configuration. *Int. J. Hydrogen Energy* **42**, 6033–6050 (2017).

10. L. Schlapbach, A. Züttel, Hydrogen-storage materials for mobile applications. *Nature* **414**, 353–358 (2001).

11. U. Eberle, M. Felderhoff, F. Schüth, Chemical and physical solutions for hydrogen storage. *Angew. Chem. Int. Ed.* **48**, 6608–6630 (2009).

12. M. Yadav, Q. Xu, Liquid-phase chemical hydrogen storage materials. *Energy Environ. Sci.* **5**, 9698–9725 (2012).

13. T. C. Johnson, D. J. Morris, M. Wills, Hydrogen generation from formic acid and alcohols using homogeneous catalysts. *Chem. Soc. Rev.* **39**, 81–88 (2010).

14. D. R. Palo, R. A. Dagle, J. D. Holladay, Methanol steam reforming for hydrogen production. *Chem. Rev.* **107**, 3992–4021 (2007).

15. M. Nielsen, E. Alberico, W. Baumann, H.-J. Drexler, H. Junge, S. Gladiali, M. Beller, Low-temperature aqueous-phase methanol dehydrogenation to hydrogen and carbon dioxide. *Nature* **495**, 85–98 (2013).

16. R. E. Rodríguez-Lugo, M. Trincado, M. Vogt, F. Tewes, G. Santiso-Quinones, H. Grützmacher, A homogeneous transition metal complex for clean hydrogen production from methanol–water mixtures. *Nat. Chem.* **5**, 342–347 (2013).

17. L. Lin, W. Zhou, R. Gao, S. Yao, X, Zhang, W. Xu, S. Zheng, Z. Jiang, Q. Yu, Y.-W. Li, C. Shi, X.-D. Wen, D. Ma, Low-temperature hydrogen production from water and methanol using Pt/α-MoC catalysts. *Nature* **544**, 80–83 (2017).

18. L. E. Heim, N. E. Schlörer, J.-H. Choi, M. H. G. Prechtl, Selective and mild hydrogen production using water and formaldehyde. *Nat. Commun.* **5**, 3621 doi: 10.1038/ncomms4621 (2014).

19. M. Trincado, V. Sinha, R. E. Rodriguez-Lugo, B. Pribanic, B. de Bruin, H. Grützmacher, Homogeneously catalysed conversion of aqueous formaldehyde to H_2 and carbonate. *Nat. Commun.* **8**, 14990 doi: 10.1038/ncomms14990 (2017).

20. D. Mellmann, P. Sponholz, H. Junge, M. Beller, Formic acid as a hydrogen storage material – development of homogeneous catalysts for selective hydrogen release. *Chem. Soc. Rev.* **45**, 3954–3988 (2016).

21. A. Boddien, D. Mellmann, F. Gärtner, R. Jackstell, H. Junge, P. J. Dyson, G. Laurenczy, R. Ludwig, M. Beller, Efficient dehydrogenation of formic acid using an iron catalyst. *Science* **333**, 1733–1736 (2011).

22. J. F. Hull, Y. Himeda, W.-H. Wang, B. Hashiguchi, R. Periana, D. J. Szalda, J. T. Muckerman, E. Fujita, Reversible hydrogen storage using CO_2 and a proton-switchable iridium catalyst in aqueous media under mild temperatures and pressures. *Nat. Chem.* **4**, 383–388 (2012).

23. R. H. Crabtree, Nitrogen-containing liquid organic hydrogen carriers: progress and prospects. *ACS Sustainable Chem. Eng.* **5**, 4491–4498 (2017).

24. P. Preuster, C. Papp, P. Wasserscheid, Liquid organic hydrogen carriers (LOHCs): toward a hydrogen-free hydrogen economy. *Acc. Chem. Res.* **50**, 74–85 (2017).

25. E. Gianotti, M. Taillades-Jacquin, J. Rozière, D. J. Jones, High-purity hydrogen generation via dehydrogenation of organic carriers: a review on the catalytic process. *ACS Catal.* **8**, 4660–4680 (2018).

26. P. T. Aakko-Saksa, C. Cook, J. Kiviaho, T. Repo, Liquid organic hydrogen carriers for transportation and storing of renewable energy – review and discussion. *J. Power Sources* **396**, 803–823 (2018).

27. Fuell Cells and Hydrogen Joint Undertaking (FCH2 JU) Governing Board. Multi-Annual Work Plan 2014−2020; FCH2 JU: Brussels, Belgium (2014).

28. DOE Technical Targets for Onboard Hydrogen Storage for Light-Duty Vehicles; U.S. DOE: Washington, D.C. (2016).

29. G. P. Pez, A. R. Scott, A. C. Cooper, H. Cheng, F. C. Wilhelm, A. H. Abdourazak, Hydrogen storage by reversible hydrogenation of pi-conjugated substrates. U.S. Patent 7351395B1 (2008).

30. A. Moores, M. Poyatos, Y. Luo and R. H. Crabtree, Catalysed low temperature H_2 release from nitrogen heterocycles. *New. J. Chem.* **2006**, *30*, 1675-1678.

31. R. Yamaguchi, C. Ikeda, Y. Takahashi, K.-i. Fujita, Homogeneous catalytic system for reversible dehydrogenation-hydrogenation reactions of nitrogen heterocycles with reversible interconversion of catalytic species. *J. Am. Chem. Soc.* **131**, 8410–8412 (2009).

32. K.-i. Fujita, T. Wada, T. Shiraishi, Reversible interconversion between 2,5-dimethylpyrazine and 2,5-dimethylpiperazine by iridium-catalyzed hydrogenation/dehydrogenation for efficient hydrogen storage. *Angew. Chem. Int. Ed.* **56**, 10886–10889 (2017).

33. C. Gunanathan, Y. Ben-David, D. Milstein, Direct synthesis of amides from alcohols and amines with liberation of H_2. *Science* **317**, 790-792 (2007).

34. P. Hu, E. Fogler, Y. Diskin-Posner, M. A. Iron, D. Milstein, A novel liquid organic hydrogen carrier system based on catalytic peptide formation and hydrogenation. *Nat. Commun.* **6**, 6859 doi: 10.1038/ncomms7859 (2015).

35. P. Hu, Y. Ben-David, D. Milstein, Rechargeable hydrogen storage system based on the dehydrogenative coupling of ethylenediamine with ethanol. *Angew. Chem. Int. Ed.* **55**, 1061–1064 (2016).

36. A. Kumar, T. Janes, N. A. Espinosa-Jalapa, D. Milstein, Selective hydrogenation of cyclic imides to diols and amines and its application in the development of a liquid organic hydrogen carrier. *J. Am. Chem. Soc.* **140**, 7453–7457 (2018).

37. J. Kothandaraman, S. Kar, R. Sen, A. Goeppert, G. A. Olah, G. K. S. Prakash, Efficient reversible hydrogen carrier system based on amine reforming of methanol. *J. Am. Chem. Soc.* **139**, 2549–2552 (2017).

38. S. Rebsdat, D. Mayer, "Ethylene Glycol" in *Ullmann's Encyclopedia of Industrial Chemistry* (Wiley-VCH, Weinheim, 2005), pp. 531–546.

39. H. Yue, Y. Zhao, X. Ma, J. Gong, Ethylene glycol: properties, synthesis, and applications. *Chem. Soc. Rev.* **41**, 4218–4244 (2012).

40. A. Wang, T. Zhang, One-pot conversion of cellulose to ethylene glycol with multifunctional tungsten-based catalysts. *Acc. Chem. Res.* **46**, 1377–1386 (2013).

41. R. D. Cortright, R. R. Davda, J. A. Dumesic, Hydrogen from catalytic reforming of biomass-derived hydrocarbons in liquid water. *Nature* **418**, 964–967 (2002).

42. G. W. Huber, J. W. Shabaker, J. A. Dumesic, Raney Ni-Sn catalyst for H_2 production from biomass-derived hydrocarbons. *Science* **300**, 2075–2077 (2003).

43. J. Zhang, G. Leitus, Y. Ben-David, D. Milstein, Facile conversion of alcohols into esters and dihydrogen catalyzed by new ruthenium complexes. *J. Am. Chem. Soc.* **127**, 10840-10841 (2005).

44. J. Zhang, G. Leitus, Y. Ben-David, D. Milstein, Efficient homogeneous catalytic hydrogenation of esters to alcohols. *Angew. Chem. Int. Ed.* **45**, 1113–1115 (2006).

45. C. Gunanathan, D. Milstein, Applications of acceptorless dehydrogenation and related transformations in chemical synthesis. *Science* **341**, 1229712/1-11 (2013).

46. R. H. Crabtree, Homogeneous Transition metal catalysis of acceptorless dehydrogenative alcohol oxidation: applications in hydrogen storage and to heterocycle synthesis. *Chem. Rev.* **117**, 9228–9249 (2017).

47. M. Trincado, D. Banerjee, H. Grützmacher, Molecular catalysts for hydrogen production from alcohols. *Energy Environ. Sci.* **7**, 2464–2503 (2014).

Acknowledgments This research was supported by the European Research Council (ERC AdG 692775). D.M. holds the Israel Matz Professorial Chair of Organic Chemistry. Y.-Q.Z. and Y.X. acknowledge the Sustainability and Energy Research Initiative (SAERI) foundation for a research fellowship. N.v.W. is supported by the Foreign Postdoctoral Fellowship Program of the Israel

Academy of Sciences and Humanities. N.v.W thanks Dr M. Iron (department of chemical research support) for fruitful discussions regarding the DFT calculations.

Author contributions D.M. conceived and directed the project. Y.-Q.Z. and D.M. designed the experiments. Y.-Q.Z. performed and analyzed the experiments. N.v.W. performed the computational studies. A.A. carried out the pioneering studies on this project. Y.X. built the gas collecting system and provided useful discussions. Y.-Q.Z., N.v.W. and D.M. prepared the manuscript.

Competing interests The authors declare no conflicts of interest.

Correspondence and requests for materials should be addressed to D.M.